JOURNAL OF MATERIALS SCIENCE 9 (1974) 476–481

Microplasticity and fatigue of some magnesium-lithium alloys

Part 2 *Cyclic stress-strain and fatigue behaviour*

R. E. LEE,* W. J. D. JONES
Department of Mechanical Engineering, University College, London, UK

Cyclic stress-strain curves have been obtained for a series of magnesium-lithium alloys with lithium contents up to 12.5wt%. The results show that the cyclic strain hardening exponents for stresses leading to failure in excess of 10^4 cycles are similar for all the alloys, even though the structure changes from hcp to bcc with increasing lithium content. This was attributed to similar deformation processes being involved in the materials at the microstrain levels involved in high endurance fatigue. There is a tendency for the plastic strain amplitude leading to failure at a given life to increase with lithium content. The accumulated work to failure for all the materials studied increases with fatigue life.

1. Introduction

In a previous paper [1], experimental results concerning the tensile microplastic behaviour of some magnesium-lithium alloys were presented. The present paper describes the behaviour of the same alloys under cyclic stress conditions leading to failure in fatigue. Cyclic stresses which cause fatigue failure in greater than 10^4 cycles generally only involve strain at the microplastic level, where only a small proportion of the bulk of the material is suffering plastic strain. From this it might be implied that similar microplastic mechanisms may be operating under both conditions of stress and that the mechanisms themselves are structure related.

In the discussion, an attempt has been made to link the tensile and cyclic stress-strain results and to see how they can be correlated with the different crystal structures of the materials.

2. Materials and experimental procedure

Details of the materials and the preparation procedure are given elsewhere [1]. Pure magnesium and alloys containing 1.2, 4.2, 8.4 and 12.5% lithium were studied. From these materials, specimens for direct stress fatigue testing were machined, with a gauge length of 16 mm and a gauge diameter of 3.8 mm.

The fatigue tests were carried out in an Avery 7306 Midget Pulsator machine at 50 Hz. This machine has an elastic lever system driven by an eccentric to apply an alternating force to the specimen. The amplitude of the force can be varied as required by adjusting the throw of the eccentric. The load on the specimen, generated by the force, is measured by means of a loop dynamometer. Static preload in either tension or compression may be applied by means of a lead screw connected to the headstock.

Strain gauges attached both to the specimen and the loop dynamometer allowed stress and strain to be measured under dynamic conditions.

3. Results

3.1. Zero tension fatigue tests

Stress against log (life) curves were plotted for all the alloys, the whole of the stress cycle being in tension with the lowest value zero. These are shown in Fig. 1. During the course of each fatigue test there was a slow drift towards zero in the mean stress owing to a progressive extension of the specimen. The drift was more noticeable at high fatigue stresses, particularly in pure magnesium and the 12.5% lithium alloy. Despite the drift in the mean stress, the stress amplitude remained constant throughout any test. In an attempt to maintain a constant mean stress, adjustments were made at frequent intervals. At

*Now at the Department of Metallurgy and Materials Science, University of Nottingham

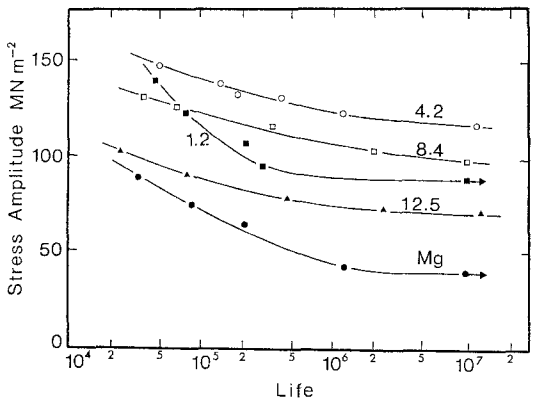

Figure 1 S/N curves in tension for the fatigue of magnesium-lithium alloys. The numbers represent the lithium content.

high stresses (short fatigue lives), the adjustment of the mean was critical in that it was found that some specimens near the end of their expected lives fractured instantaneously on attempting to reset the mean stress.

From Fig. 1, which shows the fatigue curves for the materials, it is seen that magnesium and the 1.2% lithium alloy appear to have fatigue limits in that a distinct knee appears in the curve and no failures were observed for lives in excess of 10^6 cycles. The fatigue curves for the other alloys are typical of those for materials without fatigue limits, being continuous smooth curves from low to high lives. For the purposes of comparison, the stress amplitude at 10^7 cycles was taken to be the endurance limit.

The endurance limit values for the alloys, together with the microyield stress and ultimate tensile strength values from previous experiments [1] are given in Table I. Also in the table are columns which show how much the endurance limit exceeds the microyield stress and the ratio between the endurance limit stress and the ultimate tensile strength. In order that the ratios may be compared with the published values for other materials, they should be halved. This is because, in the present tests, the peak to peak stress was recorded and not the half amplitude as in the case of most other workers. It should be noticed from these results that the endurance limit stress is considerably in excess of the microyield stress.

3.2. Cyclic tensile stress-strain behaviour

The cyclic stress-strain curve is formed by the locus of the tips of the hysteresis loops obtained when a material is subject to cyclic stresses. For the condition in which the stress varies between zero and a tensile value, the locus of the tips of the hysteresis loops coincides with the loading curve for each loop. The cyclic stress-strain curve, therefore, represents the stress-strain response of the material under equilibrium cyclic conditions. In this sense, it is the dynamic equivalent of the monotonic stress-strain curve.

Cyclic tensile stress-strain curves were plotted for the magnesium-lithium alloys by the following method. The load amplitude signal, derived from a strain gauge bonded to the dynamometer, was recorded together with the strain amplitude signal, derived from strain gauges bonded to the gauge length of the specimen. The load was increased in increments and readings of load and strain were taken after 10^3 cycles had elapsed at each new load. This was continued until strain gauge failure occurred. In the case of the 4.2, 8.4 and 12.5% lithium alloys, which showed a very marked yield behaviour, it was frequently found necessary to bond the strain gauges to the specimen after stabilization at each stress level because pre-bonded gauges were unable to withstand the large initial strains involved in yielding. The series of stress and strain points obtained for each material were plotted and joined by a smooth curve to give the cyclic stress-strain curve. These curves, together with the unidirectional stress-strain curves for

TABLE I Fatigue data for the magnesium-lithium alloys

Wt % lithium	Microyield stress (MN m^{-2})	U.T.S. (MN m^{-2})	Endurance limit (10^7) (MN m^{-2})	Endurance Limit-Microyield (MN m^{-2})	Endurance Limit U.T.S.
0	3.5	172	41	37.5	0.24
1.2	10	186	83	73	0.45
4.2	48	159	114	66	0.72
8.4	35	131	97	62	0.74
12.5	41	110	69	28	0.63

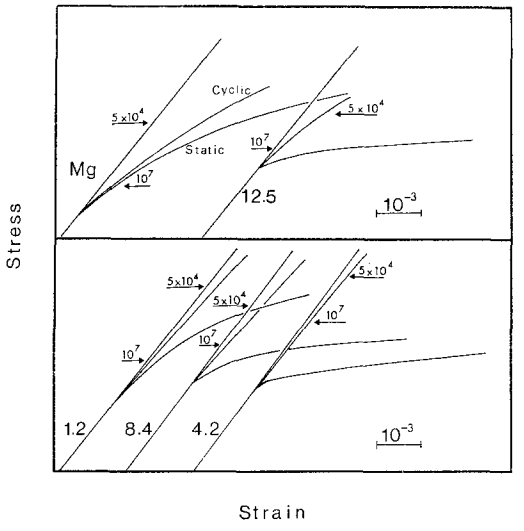

Figure 2 Tensile and cyclic stress-strain curves for magnesium-lithium alloys showing the stress levels giving lives of 10^7 and 5×10^4 cycles in fatigue.

the alloys are given in Fig. 2. The small horizontal lines on these graphs represent the stress levels which led to failure in fatigue after 5×10^4 and 10^7 cycles. The most noticeable feature of the cyclic stress-strain curves is their similar shape for all the materials in contrast to the very different unidirectional stress-strain curves. For magnesium and the 1.2% lithium alloy, fatigue failure occurs at stresses which are within the pre-yield (microplastic) region of the unidirectional stress-strain curve. On the other hand, failure in the 4.2, 8.4 and 12.5% lithium alloys occurs at stresses which led to yielding in the static stress-strain curve.

For each cyclic stress-strain curve, plastic strain amplitude values were derived for a number of stresses by subtracting the elastic strain from the total strain. Fig. 3 is a graph of log $(S - S_m)$ against log (Δe_p) for all the materials, where S is the stress amplitude, S_m the microyield stress and Δe_p the plastic strain amplitude. These plots are approximately straight lines over the range of stresses considered suggesting that there is a relationship between the stress and cyclic plastic strain amplitude of the form,

$$S - S_m = k^1(\Delta e_p)^{n^1} \qquad (1)$$

where k^1 and n^1 are constants. Elsewhere [1], experiments were described in which logarithmic plots were made of stress in excess of the micro-

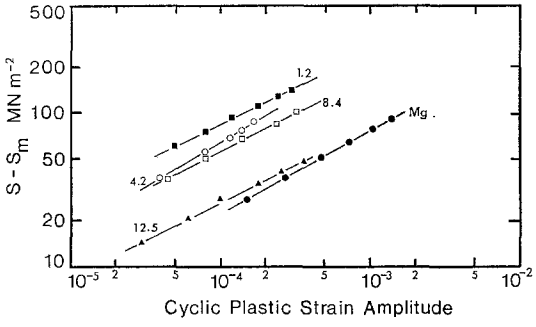

Figure 3 The cyclic stress amplitude in excess of the microyield $(S - S_m)$ plotted against the tensile cyclic plastic strain amplitude for magnesium-lithium alloys.

yield stress against plastic strain in the tensile microstrain region for the magnesium alloys. They were shown to obey a similar relationship to that given in Equation 1, from which constants equivalent to k^1 and n^1 were calculated. Table II lists the values of the constants for both the unidirectional and cyclic cases.

TABLE II Cyclic strain hardening data for magnesium-lithium alloys

Wt % lithium	Unidirectional* stress-strain microregion		Dynamic stress-strain	
	k(MN m^{-2})	n	k^1(MN m^{-2})	n^1
0	2 340	0.51	3 448	0.54
1.2	3 450	0.50	7 586	0.49
4.2	28 300	0.70	15 862	0.61
	138	0.23		
8.4	131 000	0.80	6 206	0.49
	240	0.23		
12.5	9 700	0.66	2 068	0.50
	83	0.22		

*These results were taken from Part 1 of this paper.

It is interesting to note that all the materials have very similar cyclic strain hardening exponents. For magnesium and the 1.2% lithium alloy, these values are approximately the same as those found in the microstrain region of the unidirectional stress-strain curve, whilst for the remaining alloys, the values fall between the two values obtained for the unidirectional strain hardening exponent. As all the cyclic hardening exponents are similar, the cyclic k^1 values compare the relative difficulty for alloys to undergo cyclic plastic strain. It is seen that as the lithium content is increased up to 4.2%,

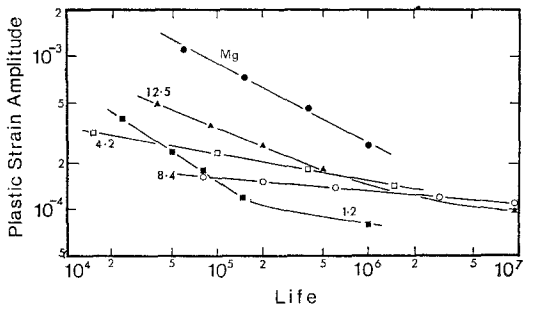

Figure 4 Plastic strain amplitude against life in tensile fatigue for magnesium-lithium alloys.

below which all the materials have an hcp structure, the k^1 values increase also. However, when the bcc structure appears in the 8.4 and 12.5% alloys the k^1 values fall indicating that it is once again easier to induce cyclic plastic strain. It is shown later that this behaviour can, to some extent, be explained in terms of the occurrence of cross-slip which, in turn, is determined by crystal structure.

Fig. 4 is a logarithmic plot of the plastic strain amplitude against the corresponding life in fatigue, assuming the plastic strain amplitude to be constant throughout the life of the specimen. It is seen that between 5×10^4 and 10^6 cycles the plots are approximately linear. This means that a relationship of the form

$$\Delta(e_p) = c(N)^d \qquad (2)$$

can exist between the plastic strain amplitude Δe_p and the life N, where c and d are constants. Table III gives the values of these constants for the alloys. Also in the tables are the measured values of the fracture strain for the materials and the predicted values of strain amplitude leading to failure in one quarter of a cycle, which is effectively the calculated fracture strain. These two values should be equal if the relationship in Equation 2 holds down to low values of N. It can be seen that for magnesium and the 1.2% lithium alloy, the experimental and calculated fracture strains are of the same order, indicating that Equation 2 may hold for these materials in the high strain fatigue region. However, the others show differences of 2 to 3 orders of magnitude.

In order to assess the relative amounts of energy absorption to failure in the materials, the plastic strain amplitude for a given life was multiplied by the cyclic $S - S_m$ value for the same life and further multiplied by the life itself to give the accumulated energy to failure. These values are plotted against life in Fig. 5. With the exception of magnesium, the total energy absorption to failure is somewhat similar for all the alloys increasing as the life increases.

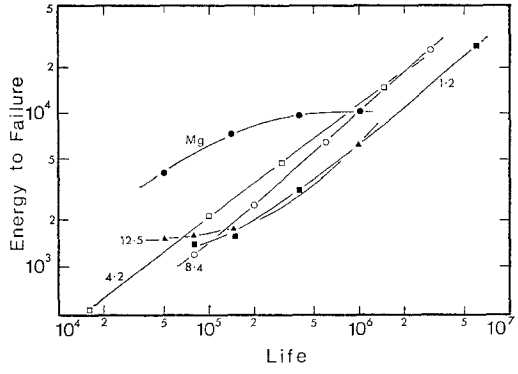

Figure 5 Accumulated energy to failure plotted against life for the tensile fatigue of magnesium-lithium alloys.

Metallographic observation of the surfaces of specimens during and after fatigue showed that with the exception of the 12.5% lithium alloy, which gave wavy slip, the resolvable slip was planar. In addition, magnesium showed a large amount of slip band extrusion formation and twinning and some slip was present as a result of stressing below the fatigue limit. In magnesium,

TABLE III Analysis of cyclic plastic strain amplitude against life curves for magnesium-lithium alloys

Wt % lithium	Constants* c	d	Experimental fracture strain	Calculated fracture strain
0	4×10^{-1}	−0.52	4.4×10^{-2}	9×10^{-1}
1.2	2.7×10^{-1}	−0.64	2.5×10^{-2}	6.5×10^{-1}
4.2	4.5×10^{-4}	−0.10	7.2×10^{-2}	5×10^{-4}
8.4	1.7×10^{-3}	−0.18	1.8	2.2×10^{-3}
12.5	2.9×10^{-2}	−0.39	2.5	5×10^{-2}

*The constants are those relating to Equation 2.

the alternating stress situation led to the operation of a twinning-untwinning process which seemed capable of absorbing large amounts of cyclic plastic strain energy.

4. Discussion

In studying the behaviour of materials under cyclic stresses, there are two main aspects to be taken account of. The first concerns the cyclic stress-strain response of the material. This indicates how the materials react to the imposition of cyclic stress and says nothing about fatigue failure as such. However, the cyclic strain against fatigue life curves indicate how the material responds to cyclic stress from the point of view of crack initiation and propagation and reflects the rate of generation and propagation of fatigue damage in the material.

Looking at the results presented earlier, there are several points which can be made arising from the response of the materials. The first is the remarkable similarity in the cyclic strain hardening exponents for all the alloys. For magnesium and the 1.2% lithium alloy, which have an hcp structure and will show predominantly planar slip, it is possible that, at the microscopic level of strain considered in these experiments, the deformation mechanism which is operating is simply dislocations running backwards and forwards between obstacles on the primary slip planes. This is likely to lead to similar strain hardening exponents both in unidirectional and cyclic straining.

The remaining alloys show cross-slip under unidirectional stressing, the presence of which in cyclic stressing has been shown by other workers [2, 3] to promote cyclic strain hardening. It is suggested that having hardened the material by the action of cross-slip, the dislocations during subsequent stress cycling may be confined to the primary slip planes as in the case of a material which does not show cross-slip. This is likely to give a cyclic strain hardening exponent which is similar to those for magnseium and the 1.2% lithium alloy, although different from those found in a unidirectional test.

In high cycle fatigue it is commonly accepted that the majority of the life is spent in initiating fatigue cracks which then spend a small proportion of the total life in propagating to failure [4]. Taking this to be the case for the materials studied here, the interpretation placed on the results can be in terms of those mechanisms which lead to fatigue crack initiation. In this sense, the plot of plastic strain amplitude against life in Fig. 4 is an indication of the ease with which fatigue damage is created in the materials. Taking a life of 2×10^5 cycles and comparing the plastic strain amplitudes it is seen that, with the exception of magnesium, an increasing plastic strain amplitude is required as the lithium content increases, and the structure changes from hcp to bcc. This may, in part, be owing to the presence of cross-slip which prevents the build up of internal stress and does not allow the notch-peak topography [5], necessary for fatigue failure initiation, to be created.

It is difficult to make comparisons with the results of other workers in this field because there is little work on fatigue hardening at such low plastic strain levels. High strain fatigue tests are usually carried out by cycling between fixed strain limits and then monitoring the accompanying stress. In the present experiments, the tests were performed between fixed stress limits and the strain monitored. The advantage of this method in the study of slip processes in fatigue is that slip is governed by the shear stresses existing on the slip planes which are, in turn, generated by the external applied stress. This means that the measured strains reflect the degree of slip activity which is occurring within the specimen.

Turning to other aspects of the fatigue of the alloys, it can be seen from the results presented in Table I that the endurance limits for the alloys in tension fatigue are, in all cases, considerably above the microyield stresses. There are two possible explanations for this. The first is that cyclic hardening occurs which raises the effective microyield stress during fatigue. However, the experiments carried out on the cyclic stress-strain characteristics of the alloys indicates that the microyield in the cyclic case is the same as that from the unidirectional stress-strain curves examined in the previous paper. The second possible explanation is that there is a certain rate of dissipation of hysteresis energy which can be tolerated by a material at a given cyclic stress level without fatigue failure being initiated. There is evidence to support this suggestion from the results for the pure magnesium. It was shown in the previous paper that after an initial period of stabilization there were stress levels at which closed hysteresis loops were obtained. The stress at which open loops were obtained under such conditions was found to be below the fatigue limit for magnesium reported

here. Similar behaviour was observed for the 1.2% lithium alloy. It was difficult to obtain conclusive results for the other alloys.

Morrow [6] suggested that, of the total amount of energy dissipated during stress cycling, the anelastic component (where stress-strain cycles lead to absorption of energy without accumulating strain in the material) may help to repair the damage created by the occurrence of permanent strain. From this idea he further suggested that fatigue failure will occur when the total energy dissipation at a given stress exceeds twice the anelastic energy at that stress. This idea was tested for magnesium and the 1.2% lithium alloy. Assuming hysteresis loops to be symmetrical in nature, the unloading portion being the loading portion in reverse, the area of loops for the endurance limit stress and the anelastic limit stress were calculated from the mathematical shape of the cyclic stress-strain curves. For magnesium, the hysteresis loop area for the endurance limit was 0.46 psi* and 0.3 psi for the hysteresis loop corresponding to the anelastic limit, the value of which is given in the previous paper. The corresponding figures for the 1.2% lithium alloy are 0.25 and 0.13 psi, respectively. The results, therefore, lend support to the suggestion of Morrow.

The present experiments show that the accumulated hysteresis energy to cause failure in fatigue, assuming the dissipation rate to be constant throughout the life, increases with the life for all the materials. A similar result was found by Halford [7] from the accumulated results of 1200 fatigue tests on a number of materials. A possible explanation arises from the work on magnesium. At the endurance limit, the major part of the hysteresis energy was involved in anelastic processes during which no cumulative strain resulted in the material. From previous experiments [1] it was found that the anelastic limit was independent of pre-stress over a large range of stresses, a fact observed by Kossowsky and Brown for iron [8]. This suggests that, even though the total energy dissipation increases with increasing stress, the anelastic contribution to the total energy remains almost constant. This means that a higher proportion of the hysteresis energy at high stress levels (i.e. low lives in fatigue) is available for creating fatigue failure. Hence, the total hysteresis energy dissipation will rise as the life increases with decreasing stress.

*1 psi = 6.89N mm^{-2}.

5. Conclusions

1. The cyclic tensile stress-strain and fatigue behaviour of some magnesium-lithium alloys with hcp and bcc structures has been studied.

2. The cyclic strain hardening exponents at the stress levels leading to failure in fatigue in excess of 10^4 cycles were found to be similar for both hcp and bcc alloys.

3. It is suggested that at the microstrain levels considered in these experiments the deformation mechanisms may be similar after the initial rapid hardening for both the hcp and bcc structure alloys. This is thought to consist mainly of the forward and reverse motion of dislocations in the primary slip planes.

4. With the exception of magnesium, the plastic strain amplitude leading to failure at a given life tends to increase with the lithium content, corresponding to a change from hcp to bcc structure.

5. The accumulated work to failure for all the materials increased with the fatigue life.

Acknowledgement

The authors are grateful to the Ministry of Technology for financial assistance in carrying out this work.

References

1. R. E. LEE and W. J. D. JONES, *J. Mater. Sci.* **9** (1974) 469.
2. C. E. FELTNER and C. LAIRD, *Acta Metallurgica* **15** (1967) 1633.
3. A. J. MCEVILY and T. L. JOHNSTON, *Int. Fracture Mech.* **3** (1967) 45.
4. W. J. PLUMBRIDGE and D. A. RYDER, *Met. Rev.* **136** (1969) 119.
5. P. J. E. FORSYTH, *Acta Metallurgica* **11** (1963) 703.
6. J. MORROW, ASTM Special Technical Publication, No. 378 (1965).
7. G. A. HALFORD, Theoretical and Applied Mechanics Report 265, University of Illinois, 1964.
8. R. KOSSOWSKY and N. BROWN, *Acta. Metallurgica* **14** (1966) 131.

Received 10 July and accepted 30 July 1973.